Induction of Caveolae in the Apical Plasma Membrane of Madin-Darby Canine Kidney Cells

Paul Verkade, Thomas Harder, Frank Lafont, and Kai Simons

European Molecular Biology Laboratory, Cell Biology and Biophysics Programme, D-69117 Heidelberg, Germany; and Max Planck Institute for Molecular Cell Biology and Genetics, Dresden, Germany

Abstract. In this paper, we have analyzed the behavior of antibody cross-linked raft-associated proteins on the surface of MDCK cells. We observed that cross-linking of membrane proteins gave different results depending on whether cross-linking occurred on the apical or basolateral plasma membrane. Whereas antibody cross-linking induced the formation of large clusters on the basolateral membrane, resembling those observed on the surface of fibroblasts (Harder, T., P. Scheiffele, P. Verkade, and K. Simons. 1998. *J. Cell Biol.* 929–942), only small (~100 nm) clusters formed on the apical plasma membrane. Cross-linked apical raft proteins e.g., GPI-anchored placental alkaline phosphatase (PLAP), influenza hemagglutinin, and gp114 coclustered and were internalized slowly (~10% after 60 min). Endocytosis occurred through surface invaginations that corresponded in size to caveolae and were labeled with caveolin-1 antibodies. Upon cholesterol depletion the internalization of PLAP was completely inhibited. In contrast, when a non-raft protein, the mutant LDL receptor LDLR-CT22, was cross-linked, it was excluded from the clusters of raft proteins and was rapidly internalized via clathrin-coated pits.

Since caveolae are normally present on the basolateral membrane but lacking from the apical side, our data demonstrate that antibody cross-linking induced the formation of caveolae, which slowly internalized cross-linked clusters of raft-associated proteins.

Key words: rafts • epithelial cells • GPI-anchored proteins • caveolin • transcytosis

Introduction

Cells employ different mechanisms to achieve lateral concentration and segregation of membrane proteins. One mechanism is the formation of microdomains in the cell membrane by lateral assemblies of sphingolipids and cholesterol, termed rafts (Simons and Ikonen, 1997; Brown and London, 1998). In some epithelial cell types, the external leaflet of the apical bilayer has a high concentration of glycosphingolipids (Simons and van Meer, 1988; Rietveld and Simons, 1998). Phosphatidylcholine is the dominant external lipid on the basolateral membrane (Simons and Fuller, 1985; van Meer, 1989). However, this membrane also contains raft lipids (Scheiffele et al., 1998; Benting et al., 1999; for reviews see Verkade and Simons, 1997; Rietveld and Simons, 1998). Recent data indicate that the raft domains in live cells are smaller than 70 nm in size (Friedrichson and Kurzchalia, 1998; Varma and Mayor, 1998).

Caveolae are specialized raft domains which consist of 50–80-nm flask-shaped membrane invaginations thought to function in endocytosis and signal transduction (Lisanti et al., 1994; Parton, 1996; Gilbert et al., 1999). They can exist as a single structure or form extensive networks of interconnected structures (see Parton, 1996). Caveolae contain a striated coat, which may represent caveolin complexes visible using scanning electron microscopic techniques (Peters et al., 1985). In MDCK cells caveolin-1 and -2 have been identified on basolateral caveolae (Scheiffele et al., 1998), but caveolae are absent from the apical plasma membrane (Vogel et al., 1998). Caveolin-1 tightly binds cholesterol (Murata et al., 1995) and can oligomerize into large protein complexes (Monier et al., 1995; Scheiffele et al., 1998). In this way caveolin-1 probably functions as a raft organizer.

Influenza virus hemagglutinin (HA)[1] and glycosyl phosphatidyl inositol (GPI)–anchored proteins were the first

Address correspondence to Kai Simons, European Molecular Biology Laboratory, Cell Biology and Biophysics Programme, Meyerhofstrasse 1, D-69117 Heidelberg, Germany. Tel.: 49-6221-387330. Fax: 49-6221-387512. E-mail: simons@embl-heidelberg.de

[1]*Abbreviations used in this paper:* CD, methyl-β-cyclodextrin; DIG, detergent-insoluble glycolipid enriched complexes; FRET, fluorescence resonance energy transfer; GPI, glycosyl-phosphatidyl-inositol; HA, hemagglutinin; LCM, low carbonate medium; LDLR, low-density lipoprotein receptor; PLAP, placental alkaline phosphatase.

proteins known to be associating with rafts (Skibbens et al., 1989; Brown and Rose, 1992). It was demonstrated that HA and GPI-anchored proteins are soluble in Triton X-100 at 4°C after synthesis in the ER but become insoluble after entering the Golgi complex and remain insoluble thereafter. Further studies (Schroeder et al., 1994) suggested that it is the interaction between lipids having saturated hydrocarbon chains like sphingolipids that governs detergent insolubility. The sphingolipid-cholesterol rafts form liquid-ordered phases separating from the liquid-disordered matrix dominated by exoplasmic unsaturated PC molecules (Brown and London, 1997). Cholesterol seems to play an essential role in the formation of the raft domains; depletion of cholesterol abolishes the resistance of raft proteins to Triton X-100 solubilization at 4°C (Cerneus et al., 1993; Scheiffele et al., 1998; Lafont et al., 1998; Keller and Simons, 1998). Therefore, detergent insolubility together with cholesterol depletion are now generally used as the criteria and as tools to study the association of proteins with rafts (Harder and Simons, 1997). Several other transmembrane proteins have also been found in the so-called detergent-insoluble, glycolipid-enriched complexes (DIGs; Fiedler et al., 1993; Sargiacomo et al., 1993; Danielsen and van Deurs, 1995; Melkonian et al., 1995). Doubly acylated tyrosine kinases of the src family, residing in the cytoplasmic leaflet of the lipid bilayer, form another important group of proteins that has been postulated to associate with sphingolipid-cholesterol rafts (Resh, 1994; Casey, 1995; Harder et al., 1998).

Lipid rafts have been postulated to play a role, by forming platforms, in the transport of proteins from the TGN to the apical plasma membrane in MDCK cells (Simons and Ikonen, 1997). Lipid rafts are also routed basolaterally from the Golgi complex but transport in the apical direction is thought to be the main pathway and involves specific clustering of rafts into apical transport containers (Verkade and Simons, 1997). Cholesterol depletion blocks apical transport but leaves the basolateral pathway operating (Keller and Simons, 1998). The role of lipid rafts in endocytosis is less studied and understood but one postulated internalization pathway involves caveolae (Parton, 1996; Gilbert et al., 1999). These surface invaginations can be internalized in a regulated fashion in fibroblasts (Parton et al., 1994) and are also engaged in transcytosis in endothelial cells (Predescu et al., 1998). Clathrin-coated pits are formed at the apical surface and endocytosed, albeit at a slower rate than from the basolateral surface (Gottlieb et al., 1993; Jackman et al., 1994; Naim et al., 1995; Shurety et al., 1996, 1998). In this paper, we have studied the behavior of antibody cross-linked raft markers. We show that antibody cross-linking at the apical plasma membrane induced formation of small raft clusters, which are slowly internalized via caveolar-like structures, a part of which can transcytose to the basolateral side.

Materials and Methods

Cell Culture and Virus Infection

MDCK strain II cells stably expressing the GPI-anchored PLAP (Brown et al., 1989) or a mutant protein of the low density lipoprotein receptor (LDLR-CT22; Matter et al., 1992) were seeded on Transwell™ filters (Costar) and grown for 3–4 d to confluence as described by Pimplikar et al. (1994). Experiments performed on gp114 were done in both cell lines and gave the same results. MDCK cells were infected overnight with adenovirus containing the nonglycosylated GPI-anchored form of the rat growth hormone (rGH0; see Benting et al., 1999) or with influenza virus strain PR8 as described (Matlin and Simons, 1983; Bennett et al., 1988).

Antibodies

Monoclonal antibodies against human PLAP were from Dako, Denmark. Rabbit polyclonal antibodies were from Dako, Denmark, or were raised against human PLAP (Sigma) and purified on a protein A column. The monoclonal antibody 4.6.5 against the 114-kD sialoglycoprotein was used as a culture supernatant (Balcarova-Ständer et al., 1984). Monoclonal (C7; Matter et al., 1992) and polyclonal antibodies (Russell et al., 1984, recognizing only the nonreduced form of the receptor) were used against LDLR. The polyclonal antibody N20 against caveolin-1 was from Santa Cruz International. Polyclonal antibodies were used against annexin XIIIb (Lafont et al., 1998). Polyclonal antibodies against clathrin were from S. Corvera (University of Massachusetts, Worcester, MA). Monoclonal antibodies against influenza hemagglutinin (HA, antibody H17L10) were prepared as described (Matlin et al., 1981). Rabbit polyclonal antibodies against rGH were from Biogenesis. Anti-rabbit and -mouse IgGs coupled to FITC or rhodamine were from Dianova. Anti-rabbit and -mouse IgGs coupled to colloidal gold were from Jackson ImmunoResearch. Iodinated anti-mouse antibodies were from Amersham. Anti-mouse and rabbit antibodies coupled to peroxidase were from Biorad. Anti-rabbit antibodies coupled to biotin and extravidin coupled to 10-nm gold were from Sigma.

Antibody Cross-linking

Complete filter holders with cells were rinsed in ice-cold phosphate buffered saline (PBS) containing 0.9 mM calcium, 1 mM magnesium and 0.2% BSA (PBS^{++}) and incubated at the apical and/or basolateral side with primary antibodies diluted in PBS^{++} at 4–8°C for 1–3 h. After rinsing in ice-cold PBS^{++} the filters were incubated at the apical and/or basolateral side with anti-rabbit or mouse IgGs coupled to biotin, a fluorochrome, gold, or ^{125}I for 1–3 h at 4–8°C. The filters were rinsed extensively in PBS^{++} and incubated at 37°C for the required time. Thereafter, the filters were put in ice-cold PBS^{++} to stop the uptake and fixed or left on ice until the end of the experiment. For immunogold double labeling experiments the cross-linking procedure was performed either with a mixture of monoclonal and polyclonal antibodies or in two consecutive rounds of cross-linking with extensive rinsing between the rounds.

The influence of cholesterol using methyl-β-cyclodextrin (CD, 10 mM) on the uptake was investigated. For this purpose the filters were incubated with the drug in minimal essential medium containing 20 mM Hepes and 15 mg/ml methionine for 1 h at 37°C on both sides before the cross-linking experiments and only from the basal side or both sides during the experiment.

Control filters were subjected to the same procedures with the omission of antibodies or drugs.

Radioactive Assay

For radioactive biochemical measurements the filters were cut from the holder after the antibody cross-linking. To release plasma membrane bound antibodies the filters were incubated with 100 mM citric acid, 140 mM NaCl, pH 2.1, for 5–10 min at 4°C while shaking. The filter was taken from the acid wash medium and from both the filter (internalized antibody) and the acid wash medium (plasma membrane bound antibody) the c.p.m. were measured. The percentage internalization was calculated as the c.p.m. measured on the filter divided by the sum of the c.p.m. on the filter and in the acid wash medium multiplied by 100. At time 0 min after internalization (when no internalization has occurred) background values of $<2\%$ were found. These background values were subtracted from the measurements.

Floatation

Control (without antibody cross-linking) or antibody-cross-linked cells were scraped from the filter in 500 μl PBS at 4°C. The cells were pelleted and lysed for 20 min on ice in 200 μl lysis buffer (0.05 M Tris, 150 mM NaCl, 2 mM EDTA, 2 mM DTT, 2% Triton X-100, 10% sucrose, and protease inhibitors). The samples were mixed with 500 μl 60% Optiprep (fi-

nal concentration 43% wt/vol). They were then overlaid with 300 μl of 35, 30, 25, 20, and 0% Optiprep in lysis buffer and spun in a TLS55 rotor for 2.5 h at 250,000 *g* at 4°C. 300-μl fractions were collected and TCA precipitated. The samples were washed with ice-cold acetone, pelleted, and air-dried. The samples were then processed for SDS-PAGE (7.5% acrylamide) and Western blotting. SDS-PAGE samples for the detection of LDLR-CT22 were incubated for 30 min at 37°C without any reducing agent (DTT) while other samples were incubated for 5 min at 95°C in the presence of DTT. The blots were incubated with primary and peroxidase-coupled secondary antibodies and detected with ECL (Amersham).

Immunolabeling Experiments

Immunofluorescence experiments and epon embedding were done as described by Harder et al. (1998) and processing for cryoimmuno EM basically as described in Scheiffele et al. (1998). As blocking solution 200 mM glycine in PBS was used and the antibodies were diluted in 0.5% BSA and 0.2% cold water fish skin gelatin in PBS.

Analysis of Raft Association

To investigate whether proteins are associated to rafts we developed an electron microscopical analysis. After an antibody cross-linking experiment, the filters were embedded in epon or processed for immunocryo EM. On negatives taken from these experiments the distance of the protein of interest (marked by gold particles) was measured to the nearest gold particle of the reference protein (cross-linked PLAP or LDLR-CT22). If a gold particle was >500 nm from the nearest gold particle this was marked as 500 nm. A minimal number of 124 gold particles was analyzed for each condition. From these data a mean distance + SEM were calculated from the raw data and for representation the distances were divided into 10 categories of 50 nm. The percentages in each category were calculated. Differences were statistically investigated with a Wilcoxon signed rank test using Statview© 5. It is noteworthy that in all these experiments we chose the dilutions of the PLAP and LDLR antibodies such that the labeling densities for PLAP and LDLR-CT22 were about the same since the distance between gold particles is very dependent on the density of these marker gold particles.

Results

One of the most remarkable ultrastructural differences between the apical and basolateral plasma membranes in polarized MDCK cells is the absence of caveolae from the raft-enriched apical membrane (Vogel et al., 1998). Cross-linked raft markers have frequently been described to move into caveolae (Mayor et al., 1994; Fujimoto, 1996; Wu et al., 1997). Thus, we decided to study the behavior of antibody cross-linked raft-associated proteins at the apical membrane. For this purpose, we used proteins with different raft affinities in an assay where proteins were cross-linked by antibodies and internalized. We have recently demonstrated that an antibody cross-linking technique can be used to study the association of proteins to rafts at the light microscopical level in BHK cells (Harder et al., 1998). We showed that raft proteins such as GPI-anchored PLAP and HA formed clusters that almost completely colocalized upon antibody cross-linking, while PLAP clusters and clusters formed by the non-raft protein LDLR or transferrin receptor segregated. As a first step we determined how our marker proteins behaved according to the Triton-insolubility criterion. Density floatation experiments of cold Triton X-100 solubilized control cells showed that PLAP floated to low density in Optiprep gradients (Fig. 1). When PLAP was cross-linked using antibodies with and without internalization for 1 h at 37°C, it floated in the same way as in untreated cells. We used the mutant LDL receptor LDLR-CT22 as a non-raft protein marker. The basolateral targeting signal is mutated in LDLR and is transported to the apical plasma membrane from where it can be endocytosed (Matter et al., 1992). LDLR-CT22 is Triton-soluble in control and antibody cross-linked conditions and stayed in the bottom fractions (Fig. 1). Gp114 is an integral membrane glycoprotein (Brändli et al., 1990; Le Bivic et al., 1990) that is mainly present at the apical membrane but can transcytose between the apical and basolateral membrane. In untreated cells, gp114 also behaved as a Triton-soluble protein (Fig. 1). In addition to the 114-kD protein, the antibodies against gp114 also recognized a 55-kD protein, which is a possible cleavage product of the 114-kD protein (Le Bivic et al., 1993). Upon antibody cross-linking the floatation pattern of gp114 changed. A minor fraction (5–10%) of the 114- and 55-kD protein floated to lower densities. We conclude that under normal conditions gp114 is not in DIGs. However, when the protein becomes clustered a small fraction acquired raft properties according to biochemical criteria. We have not investigated the possible cleavage of the 114-kD protein to the 55-kD protein further, but the proteins displayed identical Triton X-100 insolubility. In all further experiments, we did not discriminate between the 114- and 55-kD protein and refer to them as gp114.

Antibody Cross-linking Induces Small Clusters at the Apical Plasma Membrane

From the antibody cross-linking experiments in BHK cells we had seen that large clusters were formed with a size that could reach >1 μm as determined by immunofluorescence and electron microscopy (Harder et al., 1998). To study these properties in MDCK cells we performed the antibody cross-linking experiments on the apical and basolateral membranes. PLAP, gp114, and LDLR-CT22 are almost exclusively localized to the apical plasma membrane. The nonglycosylated form of the GPI-anchored rat growth hormone (rGH0) is, however, directed both apically and basolaterally and is raft associated at both membranes (Benting et al., 1999). We could therefore directly compare the distribution of this protein on the apical and basolateral plasma membrane. Confocal analysis showed that the staining for rGH0 was punctate at the apical plasma

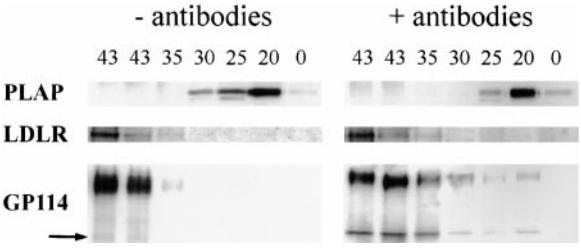

Figure 1. Triton X-100 insolubility after antibody cross-linking and internalization. Western blots from floatation gradients. Samples were taken from filter grown cells, without any treatment (− antibodies) or with antibody cross-linking and internalization for 1 h at 37°C (+ antibodies). The antibody against gp114 stains two bands on the blots; one of 114 and one of 55 kD (arrow). Percentage of Optiprep is indicated on top.

membrane without antibody cross-linking while the basolateral staining was continuous (Fig. 2, A and B). After antibody cross-linking we could not detect a change in the staining pattern of the rGH0 clusters on the apical side. On the basolateral side (Fig. 2, C and D) we observed cross-linked clusters like we had previously seen on the BHK plasma membrane (Harder et al., 1998). PLAP, gp114, and LDLR-CT22 analyzed on the apical plasma membrane gave a similar staining pattern as rGH0 before or after antibody cross-linking (data not shown). Since raft integrity is dependent on cholesterol we tested the effect of cholesterol depletion on the clustering process. Cyclodextrin (CD, 10 mM for 60 min) removes >50% of the total cholesterol content in MDCK cells (Scheiffele et al., 1998). Removal of cholesterol before antibody cross-linking did not change the staining of rGH0 on the apical side but on the basolateral side the clusters were not formed and a continuous staining was seen (Fig. 2, E and F). This difference in the formation of raft clusters on the apical and basolateral membranes is intriguing. The apical plasma membrane is, however, covered by microvilli, and in x,y-sections these may give the impression of clusters. This phenomenon complicates the analysis. We therefore adopted the antibody cross-linking assay for electron microscopical analysis. While under control conditions PLAP, rGH0, gp114, and LDLR-CT22 were distributed randomly over the apical membrane, antibody cross-linking induced the formation of small (gold) clusters (Fig. 3 A, see also Fig. 4). We measured the size of the clusters for PLAP (n = 187 clusters) and LDLR-CT22 (n = 213 clusters) and plotted them in histograms (Fig. 3 B). From these histograms we found a distribution in the size range from 30 to ~100 nm. The clusters were already formed at 4–8°C and did not increase in size after transfer to 37°C (data not shown). To ascertain that the size of the clusters was not due to the method of cross-linking, we performed control experiments. Instead of a two-step cross-linking procedure (primary and secondary antibody), a one-step (fixation and blocking after the primary antibody, n = 117 clusters) or a three-step (primary antibody, biotin-coupled secondary antibody, and a gold-coupled extravidin, n = 135 clusters) procedure was used. Amazingly, in all three cases, clusters with a maximum size of ~100 nm were formed (Fig. 3 B). The size of the clusters, therefore, seems independent of the cross-linking procedure. Cross-linking of rGH0 and gp114 also induced the formation of these small clusters (data not shown).

From our previous data we found that >80% of PLAP and HA cocluster in BHK cells (Harder et al., 1998). Therefore, we measured the distance of cross-linked HA to cross-linked PLAP clusters and divided these distances in categories of 50 nm. We found that 56% of the HA label was located within 50 nm of PLAP clusters and 80% within 100 nm of PLAP clusters (n = 105; Fig. 4 C). This resulted in a mean distance of HA towards PLAP clusters of 77.2 ± 9.9 nm (mean ± SEM). We tested whether the known raft markers caveolin-1 and annexin XIIIb, which are randomly distributed in control conditions (Lafont et al., 1998; Scheiffele et al., 1998), behaved in the same way as HA. We found that the majority of these proteins was within 100 nm of PLAP clusters (74 and 69%, caveolin-1 and annexin XIIIb, respectively, n = at least 151). Also, their mean distances to cross-linked PLAP clusters were equal to that of HA (Fig. 4, A, C, and D). We next examined how the distribution of caveolin-1 and annexin XIIIb related to LDLR-CT22 clusters. There the distribution patterns were different (78 and 80% were outside 100 nm, caveolin-1 and annexin XIIIb respectively) and this led to mean distances that were significantly different from the values obtained with the PLAP clusters (Fig. 4, B–D). When cholesterol was removed, the distribution changed (Fig. 4 C). The mean distances of caveolin-1 and annexin XIIIb to PLAP and to LDLR-CT22 were now a ~150 nm (Fig. 4 D) that is in between the control values (~100 nm to PLAP and 250 nm to LDLR-CT22). The values with CD treatment were statistically different from the values without CD treatment. Raft and non-raft proteins apparently mixed under these conditions; the apical membrane was now behaving as a homogeneous matrix. We also tested how gp114 behaved in this analysis (Fig. 4 D). The data were not statistically different from those of caveolin-1 and annexin XIIIb. Gp114 coclustered with cross-linked PLAP but not with cross-linked LDLR-CT22.

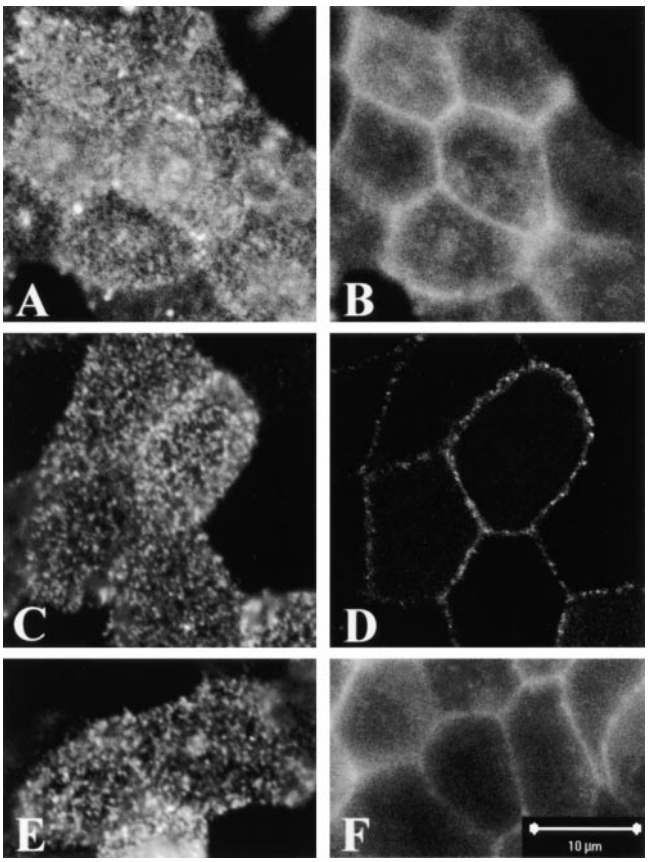

Figure 2. Antibody cross-linking of rGH0 induces basolateral clusters. x,y-confocal sections of the apical (A, C, and E) and basolateral (B, D, and F) plasma membrane of rGH0 expressing adenovirus-infected MDCK cells. Pairs A and B (without antibody cross-linking), C and D (after antibody cross-linking), and E and F (cholesterol depletion before antibody cross-linking) are from the same cells. Some parts of the apical plasma membrane are a bit out of focus since the cells are rounded up at the top. Bar, 10 μm.

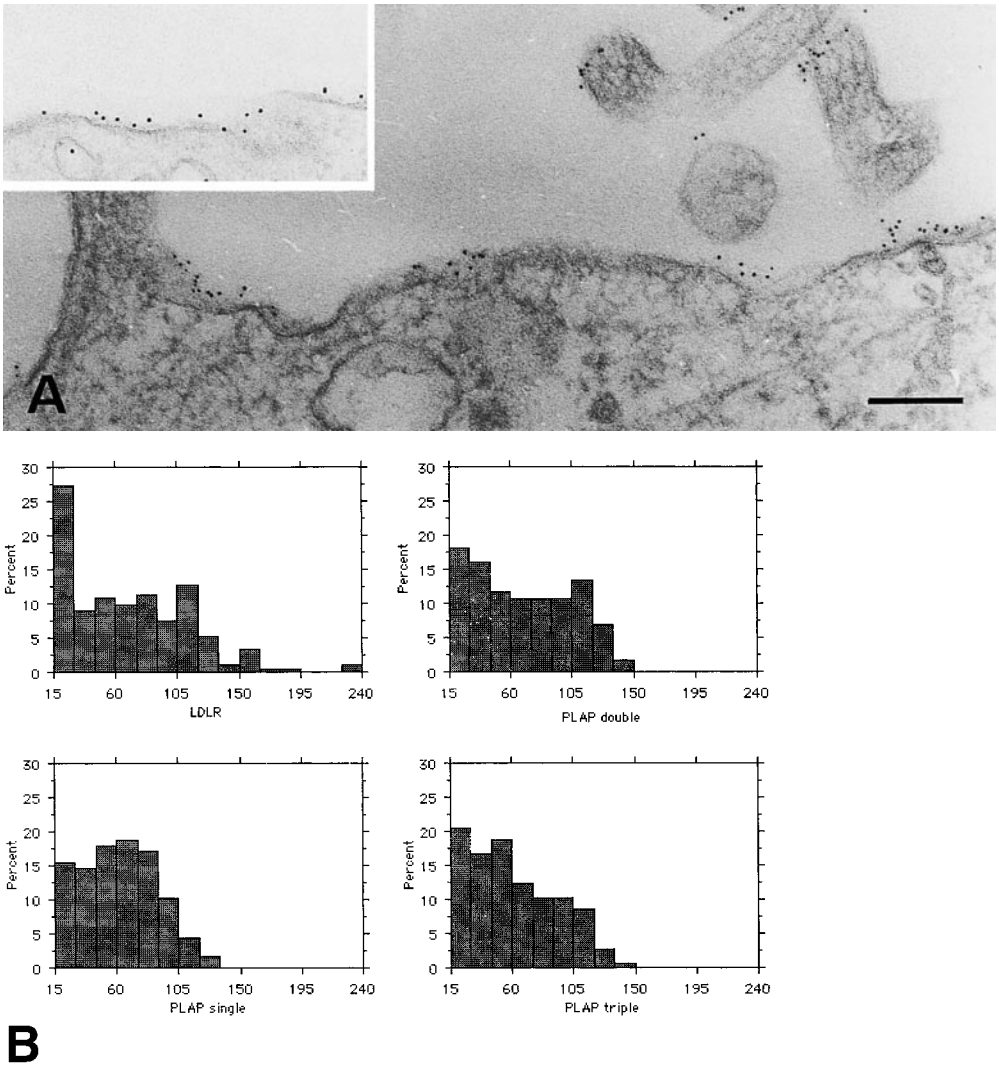

Figure 3. Antibody cross-linking of PLAP induces clusters. Electron micrographs of the apical plasma membrane of MDCK cells with and without antibody cross-linking. Antibody cross-linking of PLAP was performed with primary and 6-nm gold-coupled secondary antibodies. At the inset the distribution of PLAP is shown without antibody cross-linking (detected by 12-nm gold particles). (B) Histograms of the size distribution of gold clusters induced by the antibody cross-linking of LDLR-CT22 or PLAP (sizes on the horizontal bar are in nm). The size distribution of PLAP was measured using three different cross-linking procedures: double = primary + gold-coupled secondary antibody; single = primary antibody, fixation + blocking, gold-coupled secondary antibody; triple = primary antibody, biotin-labeled secondary antibody, gold-coupled extravidin. Bar: (A) 100 nm; (inset) 200 nm.

Clustered Raft Proteins Are Internalized Slowly via Caveolar-like Structures

Next we studied the internalization of cross-linked raft proteins from the apical plasma membrane. After cross-linking of the marker proteins at the apical surface and incubation at 37°C, we indeed observed that they were endocytosed. PLAP and gp114 were internalized slowly from the apical membrane (Fig. 5). After ~60 min, 8.6% of the PLAP and 15.5% of the gp114 were internalized when compared with the total amount of bound antibodies. This relative low rate of internalization of cross-linked PLAP and gp114 has been reported before for GPI-anchored proteins and gp114 (Le Bivic et al., 1993; Deckert et al., 1996; Mayor et al., 1998). After 60 min of endocytosis and exocytosis (through recycling and/or transcytosis) the proteins have reached steady-state equilibrium (Fig. 5). LDLR-CT22 was internalized much faster and reached a maximum of ~70% between 20 and 30 min of internalization (Fig. 5).

Upon ultrastructural examination, we found that cross-linked PLAP was internalized via structures that had the morphological appearance of caveolae (Fig. 6, A and B). Other gold-labeled structures associated with the apical plasma membrane had a tubular appearance (Fig. 6 C) and inside the cell, pleiomorphic endosome-like structures (Fig. 6, D and E) were labeled. The Golgi apparatus (Fig. 6 D) and dense lysosomes were not labeled (not shown). A remarkable observation was that PLAP-associated gold label was also found in caveolar-like structures at the basolateral plasma membrane (Fig. 6, F and G). Gp114 (Fig. 7) was found in the same types of structures as PLAP with the exception that gp114 was rarely found in tubular structures at the apical membrane. The time-dependent appearance of the different types of structures was quantitated (Fig. 8). At time 0 min of internalization, we did not detect any intracellular structures labeled, only the apical plasma membrane was covered with gold clusters. After 15 min of internalization of PLAP or gp114, apical caveolar-like invaginations and cytoplasmic endocytic structures were detected. Apical tubules or the basolateral caveolar-like structures could not be seen. The apical caveolar-like invaginations reached their maximum number after 15 min amounting to ~1 caveolar profile per cell section. In comparison, we correspondingly found between 10 and 50 caveolar profiles on the basolateral side (unpublished data). The number of cytoplasmic endocytic structures

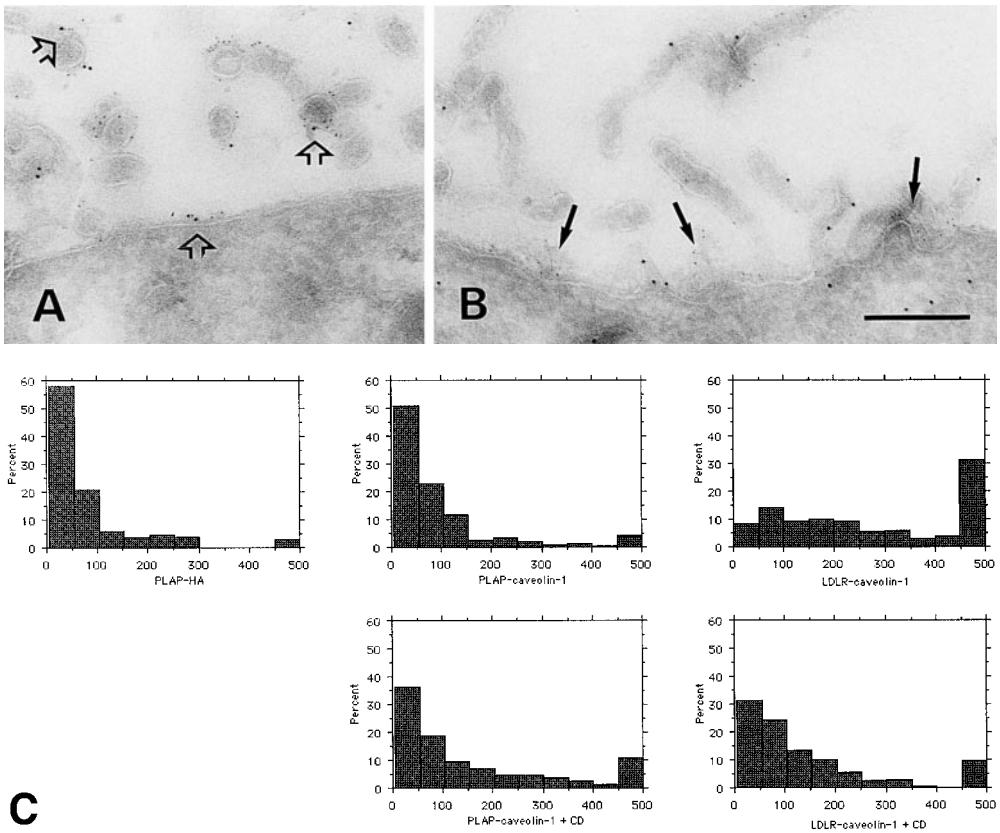

C

	PLAP		LDLR-CT22	
	-CD	+CD	-CD	+CD
HA	77.2 ± 9.9	n.d.	n.d.	n.d.
caveolin-1	95.2 ± 7.0	155.1 ± 12.7	272.8 ± 11.2	141.2 ± 9.2
annexin13B	105.7 ± 7.0	145.4 ± 10.1	238.8 ± 10.2	137.2 ± 7.2
gp114	105.9 ± 9.1	n.d.	260.3 ± 15.3	n.d.

D

Figure 4. Raft association analysis. To investigate the association of proteins to rafts the distances of gold-labeled proteins to gold cross–linked marker proteins were measured. A and B show representative cryoelectron micrographs of cross-linked PLAP (A) and LDLR-CT22 (B), both shown by the small 6-nm gold and afterwards immunolabeled for caveolin-1 (large 12-nm gold). (C) Histograms of the association of PLAP with HA and of caveolin-1 in different conditions. The distances that were measured were divided in categories of 50 nm and the percentages per category were calculated. (D) From the raw data the mean distance ± SEM in nm were calculated. Bar, 250 nm.

kept increasing from 15 to 60 min. After 60 min of internalization of PLAP, apical tubules and basolateral caveolar-like structures were detected. The basolateral membrane itself was hardly labeled. This suggests that PLAP is recycled back to the apical membrane via tubules but is also transcytosed and found in basolateral caveolae. Gp114 was also found in basolateral caveolae. However, very few apical tubules were labeled, suggesting that there is little recycling of gp114.

As expected from previous data (Matter et al., 1992), LDLR-CT22 was found in clathrin-coated invaginations labeled by clathrin antibodies at the apical membrane after cross-linking with anti-LDLR antibodies and 5 min of internalization at 37°C (data not shown). After 30 and 60 min of internalization, clathrin-coated pits and the intervening plasma membrane were rarely labeled (data not shown), indicating that most of the clustered LDLR-CT22 had been endocytosed and not recycled. Very little PLAP and gp114 was detected in clathrin-coated pits (1.1 and 2.1% of total labeled invaginations, respectively; see Fig. 7 A).

These ultrastructural data together with the internalization rates showed that the clathrin-dependent uptake of LDLR-CT22 is clearly different from the endocytosis of PLAP and gp114, the latter of which appear to employ the same internalization mechanism. This was confirmed by simultaneous internalization of PLAP and gp114 labeled with rabbit and mouse antibodies, respectively. The majority of the structures was labeled with both markers (Fig. 9). Cross-linking and internalization of PLAP or gp114 together with HA in influenza virus-infected cells also resulted in colabeling of caveolar-like and endocytic structures (data not shown). This shows that clustered raft proteins employ the same structures for internalization from the apical membrane. When gp114 and LDLR-CT22 were simultaneously internalized they were detected in different structures (Fig. 10 A). Although the internalization of clustered raft proteins on the one hand and LDLR-CT22 on the other hand use different mechanisms, they do enter the same endosome structures (Fig. 10 B). It is important to note that we never observed LDLR-CT22 in basolateral caveolae.

The Formation of Apical Caveolae Is Cholesterol Dependent

To further investigate the properties of the apical caveolar-like structures two additional features of caveolae,

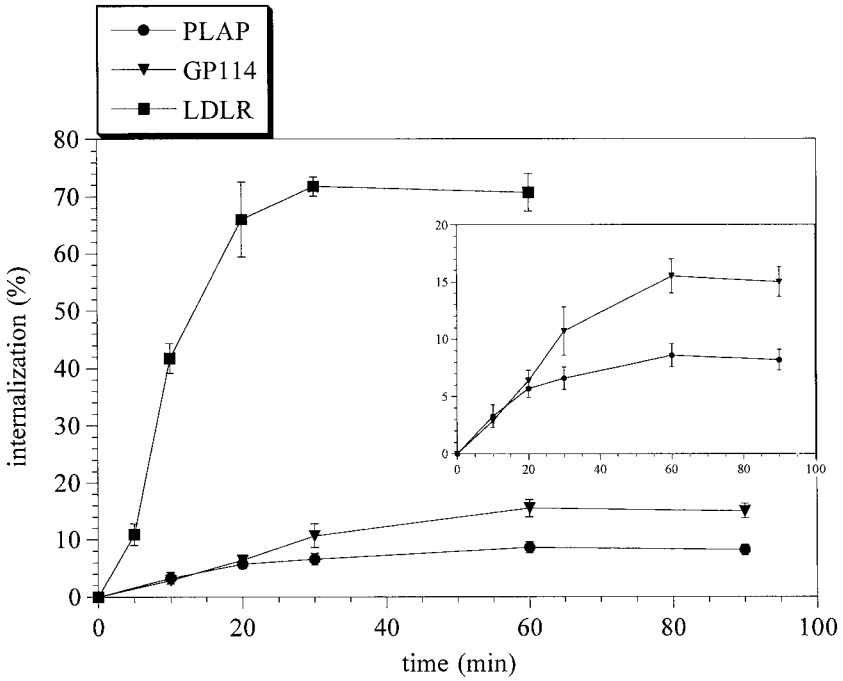

Figure 5. PLAP and gp114 endocytosis from the apical membrane. Internalization of PLAP, gp114, and LDLR-CT22 from the apical plasma membrane at 37°C measured by ^{125}I-labeled secondary antibodies (see also inset for a better view of PLAP and gp114). Numbers are expressed as percentage counts internalized compared with the total bound and internalized.

namely the presence of caveolin-1 and the dependence on cholesterol, were investigated. In previous experiments, we have detected caveolin-1 by a commercial polyclonal antibody N20 (Scheiffele et al., 1998) and did not detect any morphologically apparent caveolae at the apical membrane. Here we used the same antibody and found an accumulation of caveolin-1 in the clusters induced by PLAP cross-linking at 4–8°C (Fig. 3). When the cells were brought to 37°C and the clusters were internalized, the apical caveolar-like structures also labeled for caveolin-1 (Fig. 11 A). The PLAP-labeled, caveolar-like structures on the basolateral membrane were also identified as caveolae by their labeling with caveolin-1 (Fig. 11 B). The same results were obtained for gp114 (data not shown). Cholesterol removal reduced the uptake of PLAP to background levels (Fig. 12). If the maximum internalization was scaled to 100%, this corresponds to a reduction to <5%. The same results were obtained for gp114 (data not shown). Under the same conditions of CD treatment the internalization of LDLR-CT22 was reduced by ~50% after the cholesterol depletion (Fig. 12). Electron microscopical analysis showed that after CD treatment no caveolar-like structures were present and no gold associated to PLAP or gp114 had been internalized (data not shown). Tight junctions were intact but basolateral caveolae had disappeared in accordance with previous results (Hailstones et al., 1998). Clathrin-coated pits were still present at the apical and basolateral plasma membrane, and LDLR was still internalized via clathrin-coated pits in LDLR-CT22–expressing cells (data not shown).

Discussion

Floatation vs. Antibody Cross-linking

The generally used and accepted method to determine whether a protein is raft associated is by density gradient floatation after Triton X-100 solubilization at 4°C (Brown and London, 1997; Simons and Ikonen, 1997). Recent data demonstrated that the Triton insolubility criterion is valid for in vivo raft association (Ahmed et al., 1997; Schroeder et al., 1998). Using this method we found that the endogenous apical marker protein gp114 is weakly raft associated after cross-linking with antibodies. The association of proteins with raft domains is thought to be a dynamic phenomenon (Harder and Simons, 1997). Proteins may reside for longer or shorter periods in rafts depending on their raft affinity. It is possible that there are proteins that are raft associated in vivo but are removed by Triton extraction. Clustering of proteins may enhance raft affinity by making the protein multivalent. If gp114 has a short residence time in rafts, or if it is loosely associated, its raft association may be lost after extraction with cold Triton X-100 and floatation under normal conditions. On the other hand, under cross-linked conditions this association may be stabilized. There is, however, a difference in the extent of association with rafts in the floatation and coclustering assays. While there is only a small fraction of gp114 floating in cross-linked conditions, in the coclustering assay, the protein behaves as PLAP (and also during its subsequent internalization). The floatation and coclustering assays are based on different principles and this may cause the different outcomes. Recent experiments showed that detergent insolubility can indeed underestimate the raft association of proteins and lipids (Arni et al., 1998; Schroeder et al., 1998). We are currently studying the coclustering behavior of cross-linked proteins that do not float under normal conditions and found that the M2 protein of influenza virus behaves in the same way as gp114 (unpublished results). This protein is also routed to the apical surface of MDCK cells. The coclustering assay is thus an interesting adjunct to study the association of proteins to rafts.

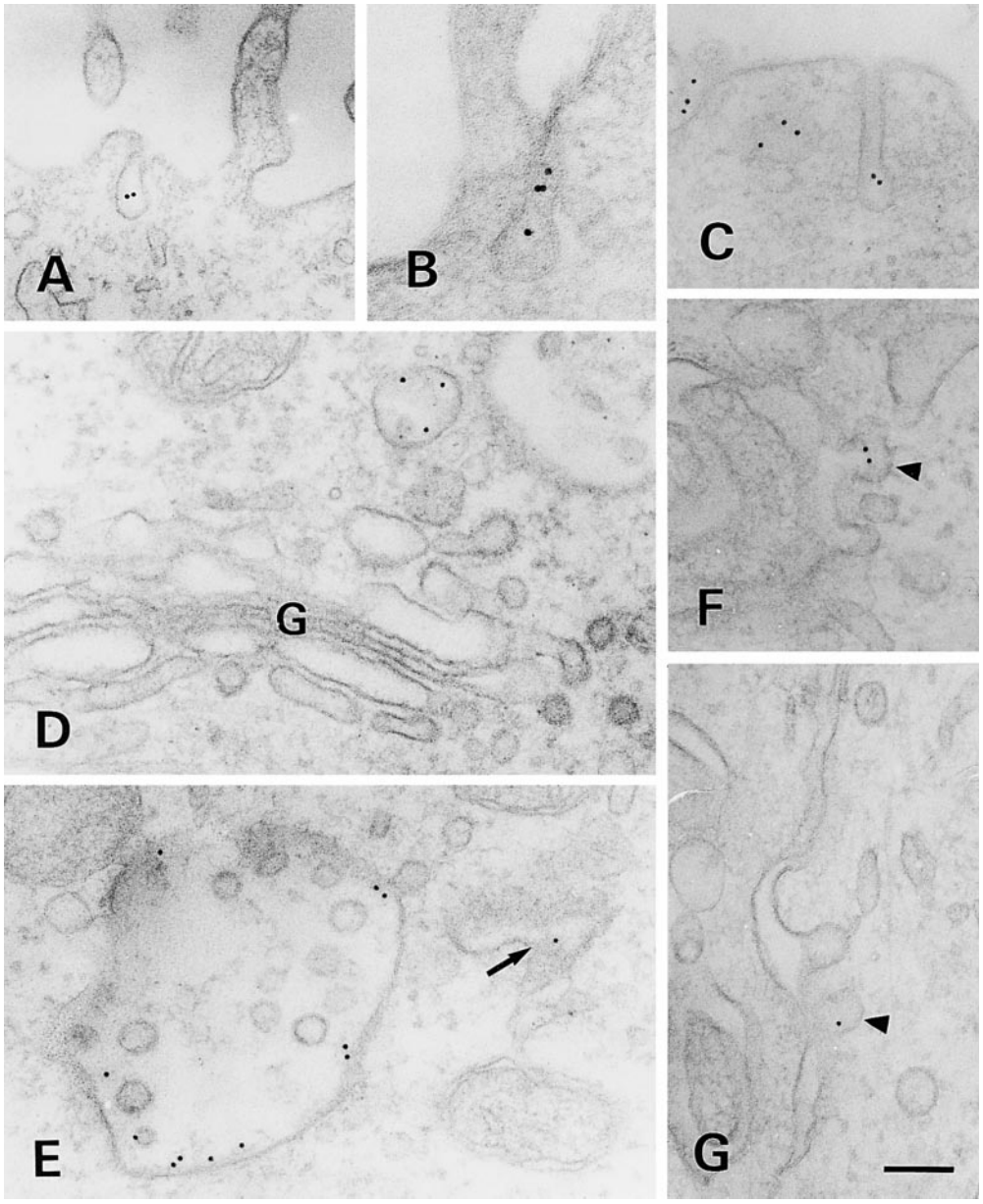

Figure 6. Electron microscopic characterization of PLAP internalizing structures. Electron micrographs of MDCK cells after 60 min internalization of PLAP at 37°C. PLAP label is shown by 12-nm gold particles. At the apical plasma membrane PLAP is detected in non-coated grape-like structures (A and B), which resemble caveolae, and in tubular structures (C). In the cytoplasm, internalized PLAP-labeled round endosomes (D) and pleiomorphic endosomes (E, arrow). The Golgi (G) is not labeled (D). At the basolateral membrane label is found in morphologically recognizable caveolae (F and G, arrowheads). Bar: (A, C–G) 100 nm; (B) 150 nm.

The Apical vs. Basolateral Plasma Membrane

The difference in behavior of raft and non-raft proteins on the apical plasma membrane of MDCK cells as compared with that seen on the basolateral membrane and to the plasma membrane of BHK cells was striking. In BHK cells, large (>1 μm) domains were formed upon cross-linking with antibodies, while in untreated cells a continuous staining pattern was observed in the light microscope (Harder et al., 1998). The same phenomenon was observed here for the basolateral plasma membrane. This is in agreement with the data that show that rafts may be very small (<70 nm) and dynamic under normal conditions (Varma and Mayor, 1998) and that antibody cross-linking induces the formation of large macrorafts. On the apical plasma membrane, where GPI-anchored proteins and glycolipids are enriched, we observed only small clusters. The cluster size was independent of the cross-linking procedure. Even three layers of cross-linking did not increase the size. This means that the underlying lipid matrix must determine the cluster size. Because of the high sphingolipid content the apical membrane is probably more tightly packed than other plasma membranes (Simons and van Meer, 1988; Brown and London, 1997). These sphingolipids together with cholesterol tend to form a liquid-ordered phase (Brown and London, 1997; Rietveld and Simons, 1998), which may lead to a reduced lateral mobility of raft constituents (Vaz and Almeida, 1993). The raft-enriched apical plasma membrane would thus be a rigid membrane compared with the fluid membrane on the basolateral side or to the plasma membrane of BHK cells, the latter of which are predominantly liquid disordered. The number of rafts on the apical plasma membrane could be so high that the liquid-ordered phase becomes continuous, i.e., the membrane would form a percolating raft

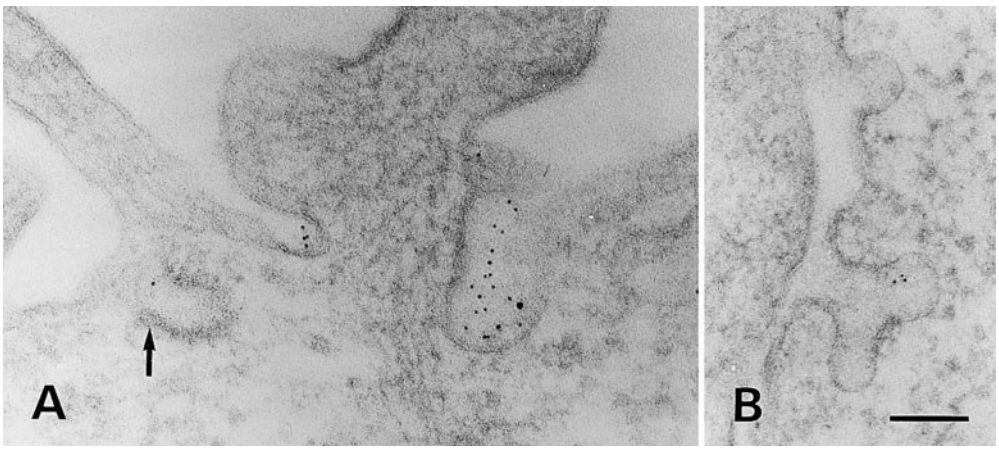

Figure 7. Electron microscopic characterization of gp114 internalizing structures. Electron micrographs of gp114 after 60 min of internalization from the apical membrane of MDCK cells. Gp114 label is shown by 6-nm gold coupled secondary antibodies. Gp114 label is found in caveolar-like structures associated with the apical plasma membrane (A). Clathrin-coated pits (A, arrow) are rarely labeled. At the basolateral membrane gp114 is also found in caveolae (B). Bar, 100 nm.

PLAP

	0 min		15 min		30 min		60 min
ACS	0.00 ± 0.00	<	1.08 ± 0.24	=	1.20 ± 0.18	=	1.44 ± 0.23
ES	0.00 ± 0.00	<	0.92 ± 0.19	<	3.24 ± 0.43	<	5.08 ± 0.56
ATS	0.00 ± 0.00	=	0.04 ± 0.04	=	0.00 ± 0.00	<	0.36 ± 0.13
BCS	0.00 ± 0.00	=	0.00 ± 0.00	=	0.00 ± 0.00	<	0.20 ± 0.50

GP114

	0 min		15 min		30 min		60 min
ACS	0.00 ± 0.00	<	1.28 ± 0.41	=	1.20 ± 0.18	=	1.32 ± 0.20
ES	0.00 ± 0.00	<	2.20 ± 0.42	=	3.44 ± 0.44	<	6.04 ± 0.71
ATS	0.00 ± 0.00	=	0.08 ± 0.06	=	0.08 ± 0.06	=	0.08 ± 0.06
BCS	0.00 ± 0.00	=	0.00 ± 0.00	=	0.04 ± 0.04	<	1.28 ± 0.31

Figure 8. Quantitation of PLAP and gp114 internalizing structures. Four types of morphologically distinct structures were quantitated at four time points. Apical caveolar-like structures (ACS): apical plasma membrane-associated structures with the characteristic 50–100-nm-round or flask-shaped morphological appearance of a single caveola or a bunch of grapes. Their width is not smaller than one-third of their length. Endocytic structures (ES): endosome-like structures appearing inside the cell. Apical plasma membrane-associated tubular structures (ATS): plasma membrane-associated tubular structures. They have a uniform form and their width is smaller than one-third of their length. Basolateral caveolar-like structures (BCS): Basolateral plasma membrane-associated structures with the characteristic 50–100-nm-round or flask-shaped morphological appearance of caveolae. Their width is not smaller than one-third of their length. The number of immunogold-labeled structures ± SEM per cell section at the given time points is given. The structures were identified on basis of their morphological criteria. 25 cell sections per time point were taken. Differences in the number of gold-labeled structures per time point were calculated with a One-way anova with three groups. In case of a significant difference, two adjacent time points were compared using a Student's *t* test or a Welch test in case variances between the groups were not equal. Differences between two time points are depicted with "=" if there was no difference, and with "<" if $P < 0.05$, indicating a significant difference.

membrane (see Fig. 1 of Vaz and Almeida, 1993). It is conceivable that if a cross-linking experiment were done on a percolating raft membrane, non-raft proteins would be hindered from forming large clusters because they are trapped in a discontinuous nonpercolating phase. Cross-linked raft proteins would only form small clusters in the percolating phase because of the rigidity of the apical plasma membrane. The segregation into large macrorafts would be driven by the ratio of raft to non-raft regions. On the more fluid basolateral plasma membrane, rafts are not continuous but move around as individual entities and are thus free to cluster into the large patches. These considerations are speculative and will need further analysis to be corroborated or not. Missing parameters are total lipid compositions for different plasma membranes and their subdomains and the determination of the percolation thresholds for different lipid compositions. Our coclustering data indicate that cross-linking of raft proteins in the apical membrane stabilizes raft domains, which coalesce into clusters in a cholesterol-dependent manner. Thus, the raft/non-raft equilibrium in the apical plasma membrane is dynamic and can be shifted towards raft stabilization by oligomerization of raft proteins, perhaps similar to that operating in the TGN during apical sorting (Benting et al., 1999). The relatively small sizes of the apical raft clusters as compared with basolateral clusters can be due to the impairment of movement in the more viscous apical plasma membrane bilayer. Alternatively, the coalescence of stabilized raft domains may be less favored due to the high density of rafts in the apical plasma membrane, which surrounds the clusters of raft proteins.

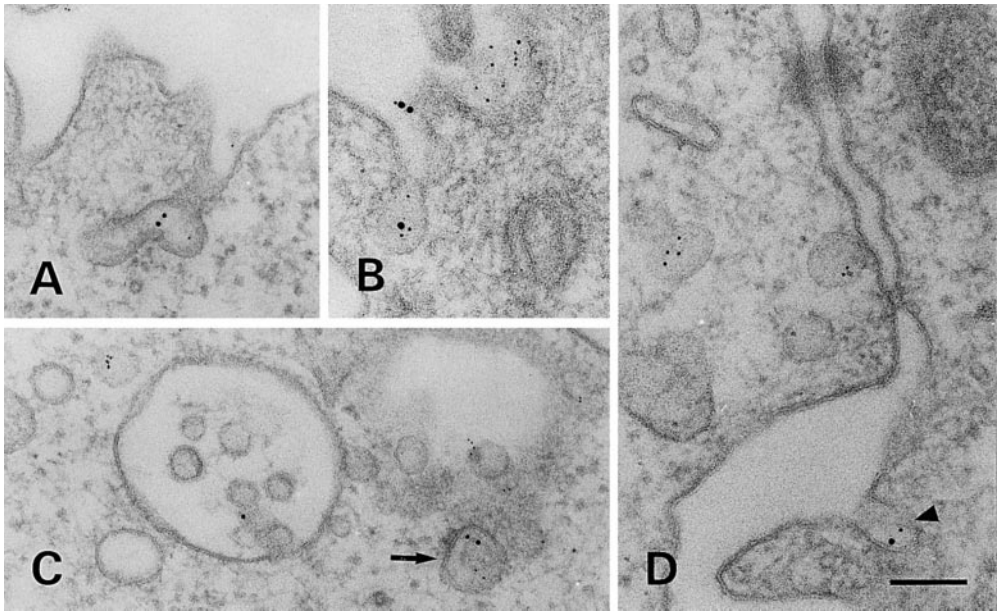

Figure 9. Simultaneous internalization of PLAP and gp114. Electron micrographs of MDCK cells after cross-linking and internalization with a mixture of polyclonal PLAP antibodies and monoclonal gp114 antibodies. The respective antibodies were detected with 12-nm gold coupled anti-rabbit antibodies and 6-nm gold coupled anti-mouse antibodies. Caveolar-like structures are double labeled at the apical plasma membrane (A an B). Not all structures are double labeled as shown in C where one endocytic structure is double labeled (arrow), while others contain one type of gold label. Basolateral caveolar-like structures are also double labeled (D, arrowhead). Bar: (A and C) 150 nm; (B and D) 100 nm.

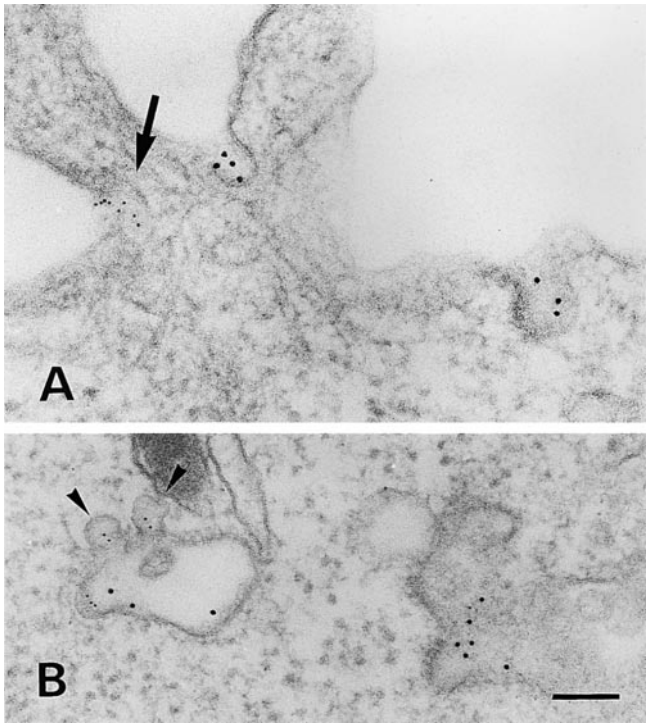

Figure 10. Internalization of LDLR-CT22 with gp114. Electron micrographs of MDCK cells after subsequent cross-linking and internalization for 1 h at 37°C of monoclonal gp114 antibodies detected with 6-nm gold-coupled anti-mouse antibodies (arrow) and monoclonal LDLR antibodies detected by 12-nm gold-coupled anti-mouse antibodies. Although both proteins are internalized via different pathways (A), they are found together in endocytic structures (B). Small structures containing only label for gp114 appear to be fusing with or pinching off from an endocytic structure (arrowheads). Bar: (A) 75 nm; (B) 100 nm.

Caveolar Endocytosis of Cross-linked Raft Proteins from the Apical Membrane

Endocytosis from the apical membrane is known to involve a clathrin-dependent pathway (Gottlieb et al., 1993; Naim et al., 1995; Rodel et al., 1999). We showed here that the non-raft protein LDLR-CT22 was internalized rapidly after antibody cross-linking via clathrin-coated vesicles. We also could demonstrate another pathway internalizing cross-linked raft proteins, including PLAP, HA, and gp114. Remarkably, this pathway seemed to involve caveolar-like invaginations. Previously, caveolae have not been identified at the apical plasma membrane (Vogel et al., 1998; Scheiffele et al., 1998). Caveolin-1, which is seemingly randomly distributed over the apical plasma membrane before antibody treatment (Scheiffele et al., 1998), becomes clustered into invaginations containing cross-linked raft proteins. In fetal intestinal cells, Danielsen and van Deurs (1995) have previously shown an 80-kD GPI-anchored protein to be internalized via 70–250-nm noncoated structures from the apical plasma membrane. Their relation to the induced apical caveolae in MDCK cells remains to be established. Cholesterol depletion completely abolished the formation of apical caveolae and blocked the internalization of the clustered raft proteins. As recently reported (Rodel et al., 1999; Subtil et al., 1999), cholesterol depletion can also affect clathrin-dependent endocytosis. The clathrin-dependent endocytosis of LDLR-CT22 from the apical side is also affected by cholesterol depletion but to a much lower extent than found for raft endocytosis (Fig. 12).

Raft clusters, stabilized by lateral cross-linking of raft-associated proteins, are thought to form platforms for signal transduction events. Many ligands are known to oligomerize their receptors on the extracellular face of the

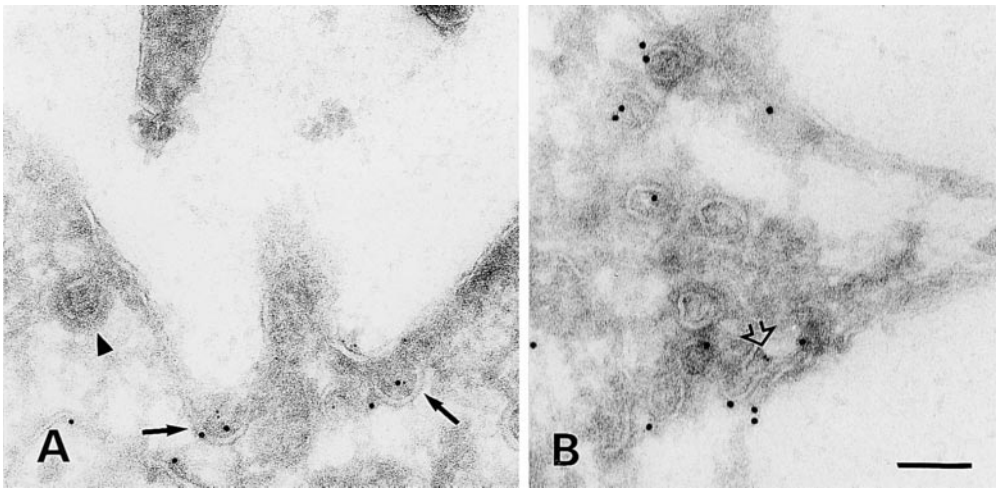

Figure 11. Distribution of caveolin-1 after internalization of PLAP. Cryoimmunoelectron micrographs of MDCK cells after a 60-min internalization of antibody cross-linked PLAP at 37°C. PLAP was further cross-linked with small 6-nm gold particles. After fixation, the cryosections were labeled for caveolin-1 (large 12-nm gold). The caveolar-like structures (arrows) at the apical plasma membrane (A) are identified as caveolae as shown by the labeling of caveolin-1. Cross-linked PLAP (open arrow) also ended up in basolateral caveolae (B). Clathrin-coated pits, identified by their electron-dense coat (arrowhead in A), are not labeled. Bar, 100 nm.

plasma membrane. A classical example, the IgE receptor FceRI is cross-linked by oligomeric antigens, generating a lipid domain enriched in gangliosides and the src-related protein tyrosine kinase Lyn (Thomas et al., 1999; Sheets et al., 1999; Pierini et al., 1996). Additionally a raft domain may be stabilized by signal-induced intracellular cross-linking of raft membrane proteins. This could either be mediated through interactions by multiple phosphotyrosine-SH2 domains or by intracellular anchoring of raft-associated membrane proteins to a matrix such as the cytoskeleton.

Caveolin-1 is present in equal amounts at the basolateral and apical membrane of MDCK cells while caveolin-2 is only present basolaterally (Scheiffele et al., 1998). We have speculated that caveolin-2 facilitates the formation of basolateral caveolae (Scheiffele et al., 1998). Only high overexpression of caveolin-1 leads to the formation of caveolae in cells lacking caveolins (Fra et al., 1995). It is possible that other proteins take the role of caveolin-2 apically. However, it is obvious that there is a constraint on the formation of caveolae on the apical side as compared with the basolateral plasma membrane and this constraint is relieved by cross-linking of raft proteins.

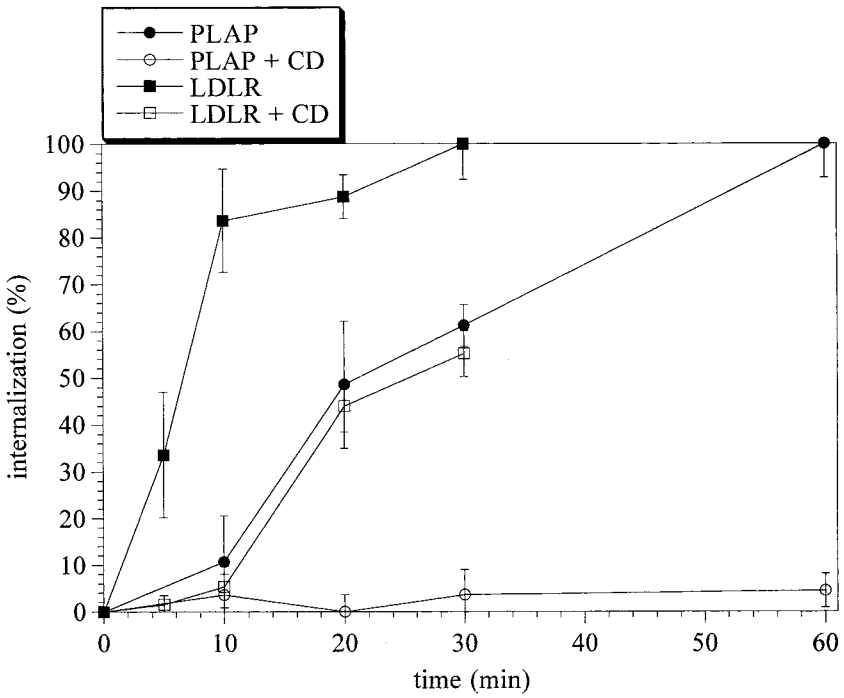

Figure 12. Cholesterol dependence of the apical internalization of PLAP and LDLR-CT22. Internalization of cross-linked PLAP and LDLR-CT22 from the apical plasma membrane at 37°C measured by ^{125}I-labeled secondary antibodies. Internalization is scaled to 100% for the maximum internalization.

Transcytosis of Cross-linked Raft Proteins

Contrary to previous results (Le Bivic et al., 1990), we detected some transcytosis of gp114 from the apical to the basolateral membrane. The amount transcytosed was ~10% of the total amount of internalized gp114 that was coupled to gold particles. For PLAP, only 2% of the internalized gold particles is transcytosed while 4% is found in the apical plasma membrane-associated tubules. These most probably represent recycling tubules (Geuze et al., 1983, 1987; Trowbridge et al., 1993; Stoorvogel et al., 1996), especially since they were found only after 60 min of internalization. Pleiomorphic endosomes underneath the apical plasma membrane were identified that, besides PLAP and gp114, also contained internalized LDLR-CT22. Recently, Mayor et al. (1998) showed that GPI-anchored proteins and receptor-mediated endocytosed proteins meet in the same endocytic compartment from which the GPI-anchored proteins are recycled back to the plasma membrane. Most likely, gp114 and PLAP are transcytosed and recycled via these endosomes.

The transcytosed raft proteins were found in caveolae at the basolateral membrane. There are conflicting reports on the normal distribution of GPI-anchored proteins on the plasma membrane. While some report a preferential localization in caveolae (Ying et al., 1992; Stahl and Mueller, 1995), others show that under normal conditions GPI-anchored proteins are diffusely distributed over the plasma membrane and that only upon cross-linking with antibodies would they move into caveolae (Mayor et al., 1994; Fujimoto, 1996; Wu et al., 1997). Although we found only single, or in a few cases two, gold particles in the basolateral caveolae, it could be that these represented small cross-linked clusters which therefore enrich in caveolae.

In conclusion, we analyzed the behavior of cross-linked raft proteins on the surface of polarized MDCK cells. Contrary to BHK cells and to the basolateral plasma membrane of MDCK cells, antibody cross-linking of raft proteins at the apical plasma membrane induced only small clusters. The stabilized raft clusters sequester caveolin-1 and induce the formation of caveolae. This concentration mechanism presents a new method to induce the formation of caveolae in membranes lacking obvious caveolae that until now was only possible by overexpression of caveolin. An important question in future studies will be to understand which signals induce the formation of apical caveolae and how the stabilization of raft domains is achieved under physiological conditions.

We thank Deborah Brown, Karl Matter, Silvia Corvera, and Jörg Heeren for cell lines and antibodies; Sigrun Brendel for expert technical assistance; Kristian Prydz for critically reading the manuscript; and the members of the Simons lab for experimental advice and discussions.

Submitted: 16 July 1999
Revised: 1 December 1999
Accepted: 5 January 2000

References

Ahmed, S.N., D.A. Brown, and E. London. 1997. On the origin of sphingolipid/cholesterol-rich detergent-insoluble cell membranes: physiological concentrations of cholesterol and sphingolipid induce formation of a detergent-insoluble, liquid-ordered lipid phase in model membranes. *Biochemistry*. 36: 10944–10953.

Arni, S., S.A. Keilbaugh, A.G. Ostermeyer, and D.A. Brown. 1998. Association of GAP-43 with detergent-resistant membranes requires two palmitoylated cysteine. *J. Biol. Chem*. 273:28478–28485.

Balcarova-Ständer, J., S.E. Pfeiffer, S.D. Fuller, and K. Simons. 1984. Development of cell surface polarity in the epithelial Madin-Darby canine kidney (MDCK) cell line. *EMBO (Eur. Mol. Biol. Organ.) J.* 3:2687–2694.

Bennett, M.A., A. Wandinger-Ness, and K. Simons. 1988. Release of putative exocytic transport vesicles from perforated MDCK cells. *EMBO (Eur. Mol. Biol. Organ.) J.* 7:4075–4085.

Benting, J.H., A.G. Rietveld, and K. Simons. 1999. N-glycans mediate the apical sorting of a GPI-anchored, raft-associated protein in Madin Darby canine kidney cells. *J. Cell Biol.* 146:313–320.

Brändli, A.W., R.G. Parton, and K. Simons. 1990. Transcytosis in MDCK cells: identification of glycoproteins transported bidirectionally between both plasma membrane domains. *J. Cell Biol.* 111:2909–2921.

Brown, D.A., B. Crise, and J.K. Rose. 1989. Mechanism of membrane anchoring affects polarized expression of two proteins in MDCK cells. *Science.* 245: 1499–1501.

Brown, D.A., and J.K. Rose. 1992. Sorting of GPI-anchored proteins to glycolipid-enriched membrane subdomains during transport to the apical cell surface. *Cell.* 68:533–544.

Brown, D.A., and E. London. 1997. Structure of detergent-resistant membrane domains: does phase separation occur in biological membranes? *Biochem. Biophys. Res. Comm*. 240:1–7.

Brown, D.A., and E. London. 1998. Functions of lipid rafts in biological membranes. *Annu. Rev. Cell Dev. Biol.* 14:111–136.

Casey, P.J. 1995. Protein lipidation in cell signaling. *Science.* 268:221–225.

Cerneus, D.P., E. Ueffing, G. Posthuma, G.J. Strous, and A. van der Ende. 1993. Detergent insolubility of alkaline phosphatase during biosynthetic transport and endocytosis. Role of cholesterol. *J. Biol Chem*. 268:3150–3155.

Danielsen, E.M., and B. van Deurs. 1995. A transferrin-like GPI-linked iron-binding protein in detergent-insoluble non-caveolar microdomains at the apical surface of fetal intestinal epithelial cells. *J. Cell Biol.* 131:939–950.

Deckert, M., M. Ticchioni, and A. Bernard. 1996. Endocytosis of GPI-anchored proteins in human lymphocytes: role of glycolipid-based domains, actin cytoskeleton, and protein kinases. *J. Cell Biol.* 133:791–799.

Fiedler, K., T. Kobayashi, T.V. Kurzchalia, and K. Simons. 1993. Glycosphingolipid-enriched detergent-insoluble complexes in protein sorting in epithelial cells. *Biochemistry.* 32:6365–6373.

Fra, A.M., E. Williamson, K. Simons, and R.G. Parton. 1995. De novo formation of caveolae in lymphocytes by expression of VIP21-caveolin. *Proc. Natl. Acad. Sci. USA*. 92:8655–8659.

Friedrichson, T., and T. Kurzchalia. 1998. Microdomains of GPI-anchored proteins in living cells revealed by chemical cross-linking. *Nature.* 394:802–805.

Fujimoto, T. 1996. GPI-anchored proteins, glycosphingolipids, and sphingomyelin are sequestered to caveolae only after crosslinking. *J. Histochem. Cytochem*. 44:929–941.

Geuze, H.J., J.W. Slot, G.J. Strous, H.F. Lodish, and A.L. Schwartz. 1983. Intracellular site of asialoglycoprotein receptor-ligand uncoupling: double-label immunoelectron microscopy during receptor-mediated endocytosis. *Cell.* 32: 277–287.

Geuze, H.J., J.W. Slot, and A.L. Schwartz. 1987. Membranes of sorting organelles display lateral heterogeneity in receptor distribution. *J. Cell Biol.* 104:1715–1723.

Gilbert, A., J-P. Paccaud, M. Foti, G. Porcheron, J. Balz, and J.-L. Carpentier. 1999. Direct demonstration of the endocytic function of caveolae by a cell-free assay. *J. Cell Sci.* 112:1101–1110.

Gottlieb, T.A., I.E. Ivanov, M. Adesnik, and D.D. Sabatini. 1993. Actin microfilaments play a critical role in endocytosis at the apical but not the basolateral surface of polarized epithelial cells. *J. Cell Biol.* 120:695–710.

Hailstones, D., L.S. Sleer, R.G. Parton, and K.K. Stanley. 1998. Regulation of caveolin and caveolae by cholesterol in MDCK cells. *J. Lipid Res.* 39:369–379.

Harder, T., and K. Simons. 1997. Caveolae, DIGs, and the dynamics of sphingolipid-cholesterol microdomains. *Curr. Opin. Cell Biol.* 9:534–542.

Harder, T., P. Scheiffele, P. Verkade, and K. Simons. 1998. Lipid domain structure of the plasma membrane revealed by patching of membrane components. *J. Cell Biol.* 141:929–942.

Jackman, M.R., W. Shurety, J.A. Ellis, and J.P. Luzio. 1994. Inhibition of apical but not basolateral endocytosis of ricin and folate in Caco-2 cells by cytochalasin D. *J. Cell Sci.* 107:2547–2556.

Keller, P., and K. Simons. 1998. Cholesterol is required for surface transport of influenza virus hemagglutinin. *J. Cell Biol.* 140:1357–1367.

Lafont, F., S. Lecat, P. Verkade, and K. Simons. 1998. Annexin XIIIb associates with lipid microdomains to function in apical delivery. *J. Cell Biol.* 142:1413–1427.

Le Bivic, A., Y. Sambuy, K. Mostov, and E. Rodriguez-Boulan. 1990. Vectorial targeting of an endogenous apical membrane sialoglycoprotein and uvomorulin in MDCK cells. *J. Cell Biol.* 110:1533–1539.

Le Bivic, A., M. Garcia, and E. Rodriguez-Boulan. 1993. Ricin-resistant Madin-Darby canine kidney cells missort a major endogenous apical sialoglycoprotein. *J. Biol. Chem*. 268:6909–6916.

Lisanti, M.P., P.E. Scherer, J. Vidugiriene, Z. Tang, A. Hermanowski-Vosatka, Y.H. Tu, R.F. Cook, and M. Sargiacomo. 1994. Characterization of caveolin-rich membrane domains isolated from an endothelial-rich source: implications for human disease. *J. Cell Biol.* 126:111–126.

Matlin, K.S., and K. Simons. 1983. Reduced temperature prevents transfer of a

membrane glycoprotein to the cell surface but does not prevent terminal glycosylation. *Cell.* 34:233–243.
Matlin, K.S., H. Reggio, A. Helenius, and K. Simons. 1981. Infectious entry pathway of influenza virus in a canine kidney cell line. *J. Cell Biol.* 91:601–613.
Matter, K., W. Hunziker, and I. Mellman. 1992. Basolateral sorting of LDL receptor in MDCK cells: the cytoplasmic domain contains two tyrosine-dependent targeting determinants. *Cell.* 71:741–753.
Mayor, S., K.G. Rothberg, and F.R. Maxfield. 1994. Sequestration of GPI-anchored proteins in caveolae triggered by cross-linking. *Science.* 264:1948–1951.
Mayor, S., S. Sabharanjak, and F.R. Maxfield. 1998. Cholesterol-dependent retention of GPI-anchored proteins in endosomes. *EMBO (Eur. Mol. Biol. Organ.) J.* 17:4626–4638.
Melkonian, K.A., T. Chu, L.B. Tortorella, and D.A. Brown. 1995. Characterization of proteins in detergent-resistant membrane complexes from Madin-Darby canine kidney epithelial cells. *Biochemistry.* 34:16161–16170.
Monier, S., R.G. Parton, F. Vogel, J. Behlke, A. Henske, and T.V. Kurzchalia. 1995. VIP21-caveolin, a membrane protein constituent of the caveolar coat, oligomerizes in vivo and in vitro. *Mol. Biol. Cell.* 6:911–927.
Murata, M., J. Peranen, R. Schreiner, F. Wieland, T.V. Kurzchalia, and K. Simons. 1995. VIP21/caveolin is a cholesterol-binding protein. *Proc. Natl. Acad. Sci. USA.* 92:10339–10343.
Naim, H.Y., D.T. Dodds, C.B. Brewer, and M.G. Roth. 1995. Apical and basolateral coated pits of MDCK cells differ in their rates of maturation into coated vesicles, but not in the ability to distinguish between mutant hemagglutinin proteins with different internalization signals. *J. Cell Biol.* 129:1241–1250.
Parton, R.G., B. Joggerst, and K. Simons. 1994. Regulated internalization of caveolae. *J. Cell Biol.* 127:1199–1215.
Parton, R.G. 1996. Caveolae and caveolins. *Curr. Opin. Cell Biol.* 8:542–548.
Peters, K.R., W.W. Carley, and G.E. Palade. 1985. Endothelial plasmalemmal vesicles have a characteristic striped bipolar surface structure. *J. Cell Biol.* 101:2233–2238.
Pierini, L., D. Holowka, and B. Baird. 1996. Fc epsilon RI-mediated association of 6-micron beads with RBL-2H3 mast cells results in exclusion of signaling proteins from the forming phagosome and abrogation of normal downstream signaling. *J. Cell Biol.* 134:1427–1439.
Pimplikar, S.W., E. Ikonen, and K. Simons. 1994. Basolateral protein transport in streptolysin O-permeabilized MDCK cells. *J. Cell Biol.* 125:1025–1035.
Predescu, D., S. Predescu, T. McQuistan, and G.E. Palade. 1998. Transcytosis of alpha1-acidic glycoprotein in the continuous microvascular endothelium. *Proc. Natl. Acad. Sci. USA.* 95:6175–6180.
Resh, M.D. 1994. Myristylation and palmitylation of src family members: the fats of the matter. *Cell.* 76:411–413.
Rietveld, A., and K. Simons. 1998. The differential miscibility of lipids as the basis for the formation of functional membrane rafts. *Biochem. Biophys. Acta.* 1376:467–479.
Rodel, S.V., G. Skretting, O. Garred, F. Vilhardt, B. van Deurs, and K. Sandvig. 1999. Extraction of cholesterol with methyl-β-cyclodextrin perturbs formation of clathrin-coated endocytic vesicles. *Mol. Biol. Cell.* 10:961–974.
Russell, D.W., W.J. Schneider, T. Yamamoto, K.L. Luskey, M.S. Brown, and J.L. Goldstein. 1984. Domain map of LDL receptor: sequence homology with the epidermal growth factor precursor. *Cell.* 37:577–585.
Sargiacomo, M., M. Sudol, Z. Tang, and M.P. Lisanti. 1993. Signal transducing molecules and GPI-linked proteins form a caveolin-rich insoluble complex in MDCK cells. *J. Cell Biol.* 122:789–807.
Scheiffele, P., P. Verkade, A.M. Fra, H. Virta, K. Simons, and E. Ikonen. 1998. Caveolin-1 and -2 in the exocytic pathway of MDCK cells. *J. Cell Biol.* 140: 795–806.
Schroeder, R., E. London, and D. Brown. 1994. Interactions between saturated acyl chains confer detergent resistance on lipids and glycosylphosphatidylinositol (GPI)-anchored proteins: GPI-anchored proteins in liposomes and cells show similar behavior. *Proc. Natl. Acad. Sci. USA.* 91:12130–12134.
Schroeder, R., S.N. Ahmed, Y. Zhu, E. London, and D. Brown. 1998. Cholesterol and sphingolipid enhance the Triton X-100 insolubility of glycosylphosphatidylinositol-anchored proteins by promoting the formation of detergent-insoluble ordered membrane domains. *J. Biol. Chem.* 273:1150–1157.
Sheets, E.D., D. Holowka, and B. Baird. 1999. Critical role for cholesterol in Lyn-mediated tyrosine phosphorylation of FcepsilonRI and their association with detergent-resistant membranes. *J. Cell. Biol.* 145:877–887.
Shurety, W., N.A. Bright, and J.P. Luzio. 1996. The effects of cytochalasin D and phorbol myristate acetate on the apical endocytosis of ricin in polarised Caco-2 cells. *J. Cell Sci.* 109:2927–2935.
Shurety, W., N.L. Stewart, and J.L. Stow. 1998. Fluid-phase markers in the basolateral endocytic pathway accumulate in response to the actin assembly-promoting drug Jasplakinolide. *Mol. Biol. Cell.* 9:957–975.
Simons, K., and S.D. Fuller. 1985. Surface polarity in epithelia. *Ann. Rev. Cell Biol.* 1:243–288.
Simons, K., and E. Ikonen. 1997. Sphingolipid-cholesterol rafts in membrane trafficking and signalling. *Nature.* 387:569–572.
Simons, K., and G. van Meer. 1988. Lipid sorting in epithelial cells. *Biochemistry.* 27:6197–6202.
Skibbens, J.E., M.G. Roth, and K.S. Matlin. 1989. Differential extractability of influenza virus hemagglutinin during intracellular transport in polarized epithelial cells and nonpolar fibroblasts. *J. Cell Biol.* 108:821–832.
Stahl, A., and B.M. Mueller. 1995. The urokinase-type plasminogen activator receptor, a GPI-linked protein, is localized in caveolae. *J. Cell Biol.* 129:335–344.
Stoorvogel, W., V. Oorschot, and H.J. Geuze. 1996. A novel class of clathrin-coated vesicles budding from endosomes. *J. Cell Biol.* 132:21–33.
Subtil, A., I. Gaidarov, K. Kobylarz, M.A. Lampson, J.H. Keen, and T.E. McGraw. 1999. Acute cholesterol depletion inhibits clathrin-coated pit budding. *Proc. Natl. Acad. Sci. USA.* 96:6775–6780.
Thomas, J.L., D. Holowka, B. Baird, and W.W. Webb. 1999. Large-scale co-aggregation of fluorescent lipid probes with cell surface proteins. *J. Cell Biol.* 125:795–802.
Trowbridge, I.S., J.F. Collawn, and C.R. Hopkins. 1993. Signal-dependent membrane protein trafficking in the endocytic pathway. *Annu. Rev. Cell Biol.* 9:129–161.
van Meer, G. 1989. Lipid traffic in animal cells. *Ann. Rev. Cell Biol.* 5:247–275.
Varma, R., and S. Mayor. 1998. GPI-anchored proteins occur in sub-micron domains at the surface of living cells. *Nature.* 394:798–801.
Vaz, W.L.C., and P.F.F. Almeida. 1993. Phase topology in multi-phase lipid bilayers: is the biological membrane a domain mosaic? *Curr. Opin. Struct. Biol.* 3:482–488.
489–505.
Verkade, P., and K. Simons. 1997. Lipid microdomains and membrane trafficking in mammalian cells. *Histochem. Cell Biol.* 108:211–220.
Vogel, U., K. Sandvig, and B. van Deurs. 1998. Expression of caveolin-1 and polarized formation of invaginated caveolae in Caco-2 and MDCK II cells. *J. Cell Sci.* 111:825–832.
Wu, C., S. Butz, Y. Ying, and R.G. Anderson. 1997. Tyrosine kinase receptors concentrated in caveolae-like domains from neuronal plasma membrane. *J. Biol. Chem.* 272:3554–3559.
Ying, Y.S., R.G. Anderson, and K.G. Rothberg. 1992. Each caveola contains multiple glycosyl-phosphatidylinositol-anchored membrane proteins. *Cold Spring Harb. Symp. Quant. Biol.* 57:593–604.